A&A 657, L16 (2022)
https://doi.org/10.1051/0004-6361/202142992

Astronomy & Astrophysics

LETTER TO THE EDITOR

Discovery of C_5H^+ and detection of C_3H^+ in TMC-1 with the QUIJOTE line survey*

J. Cernicharo[1], M. Agúndez[1], C. Cabezas[1], R. Fuentetaja[1], B. Tercero[2,3], N. Marcelino[2], Y. Endo[4], J. R. Pardo[1], and P. de Vicente[3]

[1] Grupo de Astrofísica Molecular, Instituto de Física Fundamental (IFF-CSIC), C/ Serrano 121, 28006 Madrid, Spain
e-mail: jose.cernicharo@csic.es
[2] Centro de Desarrollos Tecnológicos, Observatorio de Yebes (IGN), 19141 Yebes Guadalajara, Spain
[3] Observatorio Astronómico Nacional (OAN, IGN), Madrid, Spain
[4] Department of Applied Chemistry, Science Building II, National Chiao Tung University, 1001 Ta-Hsueh Rd., Hsinchu 30010, Taiwan

Received 23 December 2021 / Accepted 5 January 2022

ABSTRACT

We report the discovery of the C_5H^+ cation toward TMC-1 with the QUIJOTE line survey. Four lines from $J = 7 - 6$ up to $J = 10 - 9$ have been identified in perfect harmonic frequency relation that can be fit with $B = 2411.94397 \pm 0.00055$ MHz and $D = 138 \pm 3$ Hz. The standard deviation of the fit is 4.4 kHz. After discarding potential candidates, C_5H^- among them, we conclude that the carrier is C_5H^+, for which accurate ab initio calculations provide $B = 2410.3$ MHz. We also report for the first time in a cold starless core the detection of the C_3H^+ cation. The column densities we derive for C_5H^+ and C_3H^+ are $(8.8\pm0.5)\times10^{10}$ cm^{-2} and $(2.4\pm0.2)\times10^{10}$ cm^{-2}, respectively. Hence, the C_5H^+/C_3H^+ abundance ratio is 3.7 ± 0.5. The fact that C_5H^+ is more abundant than C_3H^+ is well explained by dedicated chemical models and is due to the slow reactivity of C_5H^+ with H_2, while C_3H^+ reacts with H_2.

Key words. molecular data – line: identification – ISM: molecules – ISM: individual objects: TMC-1 – astrochemistry

1. Introduction

The QUIJOTE[1] line survey of TMC-1 (Cernicharo et al. 2021a) performed with the Yebes 40 m radio telescope has permitted detection of nearly 27 new molecular species in the last months, most of them hydrocarbons and cycles, indene among them (see, e.g., Agúndez et al. 2021; Cernicharo et al. 2021b,c and references therein). QUIJOTE has now reached a level of sensitivity that permits performing rotational spectroscopy of unknown species in space. Several molecules have been detected in this source that lack previous rotational spectroscopic laboratory information. Based on spectral patterns found in the data that can be assigned to linear or asymmetric species, and with the help of a high level of theory quantum chemical calculations, we have discovered molecules such as HC_5NH^+ (Marcelino et al. 2020), HC_3O^+ (Cernicharo et al. 2020a), HC_3S^+ (Cernicharo et al. 2021d), CH_3CO^+ (Cernicharo et al. 2021e), $HCCS^+$ (Cabezas et al. 2022a), and HC_7NH^+ (Cabezas et al. 2022b).

TMC-1 and IRC+10216 are the sources in which all known C_nH^- anions in space have been detected (McCarthy et al. 2006; Cernicharo et al. 2007; Brünken et al. 2007; Kawaguchi et al. 2007; Remijan et al. 2007). Nitrile anions CN^-, C_3N^- and C_5N^- were first detected in the circumstellar envelope of IRC+10216 (Agúndez et al. 2010; Thaddeus et al. 2008; Cernicharo et al. 2008). Only with the sensitivity of QUIJOTE has it been possible to detect the anions C_3N^- and C_5N^- in TMC-1 (Cernicharo et al. 2020b). The detection of new cations and anions is an astounding source of information with which chemical models can be improved and insights into the chemical paths can be gained that lead to their formation.

In this Letter we report the discovery of four strong lines in TMC-1, with a perfect harmonic relation, that we assign to the C_5H^+ cation. The only alternative plausible candidate, C_5H^-, has been ruled out on the basis of accurate ab initio calculations and the lack of emission of these lines in IRC+10216. In addition, we report for the first time the detection of the C_3H^+ cation in a starless core. C_3H^+ was previously detected only toward PDRs (Pety et al. 2012; McGuire et al. 2014; Cuadrado et al. 2015; Gúzman et al. 2015), Sgr B2 (McGuire et al. 2013), diffuse clouds (Gerin et al. 2019), and the $z = 0.89$ source PKS 1830-211 (Tercero et al. 2020). A previous claim of detection of a line of C_3H^+ in absorption toward TMC-1 (McGuire et al. 2013) is ruled out by our sensitive QUIJOTE observations, which clearly show this line to be in emission. We use dedicated chemical models to compare the expected abundances with the observed ones and obtain excellent agreement between models and observations.

2. Observations

New receivers, built within the Nanocosmos project[2] and installed at the Yebes 40 m radiotelescope, were used for the observations of TMC-1 ($\alpha_{J2000} = 4^h41^m41.9^s$ and $\delta_{J2000} = +25°41'27''.0$). A detailed description of the system is given by Tercero et al. (2021). The receiver consists of two cold high

* Based on observations carried out with the Yebes 40 m telescope (projects 19A003, 20A014, 20D023, and 21A011). The 40 m radiotelescope at Yebes Observatory is operated by the Spanish Geographic Institute (IGN, Ministerio de Transportes, Movilidad y Agenda Urbana).
[1] *Q*-band Ultrasensitive Inspection Journey to the Obscure TMC-1 Environment.

[2] https://nanocosmos.iff.csic.es/

electron mobility transistor amplifiers covering the 31.0–50.3 GHz band with horizontal and vertical polarizations. Receiver temperatures in the runs achieved during 2020 vary from 22 K at 32 GHz to 42 K at 50 GHz. Some power adaptation in the down-conversion chains reduced the receiver temperatures during 2021 to 16 K at 32 GHz and 25 K at 50 GHz. The backends are $2 \times 8 \times 2.5$ GHz fast-Fourier transform spectrometers with a spectral resolution of 38.15 kHz providing the whole coverage of the Q band in both polarizations. All observations were performed in frequency- switching mode with frequency throws of 8 and 10 MHz. The main beam efficiency varies from 0.6 at 32 GHz to 0.43 at 50 GHz. The intensity scale used in this work, antenna temperature (T_A^*), was calibrated using two absorbers at different temperatures and the atmospheric transmission model ATM (Cernicharo 1985; Pardo et al. 2001). Calibration uncertainties were adopted to be 10%. All data were analyzed using the GILDAS package[3]. Details of the QUIJOTE line survey are provided by Cernicharo et al. (2021a). The data presented here correspond to 238 hours of observing time on the source.

3. Results

Line identification in this work was done using the catalogs MADEX (Cernicharo 2012), CDMS (Müller et al. 2005), and JPL (Pickett et al. 1998). By December 2021, the MADEX code contained 6421 spectral entries corresponding to the ground and vibrationally excited states, together with the corresponding isotopologs, of 1727 molecules.

With the current level of sensitivity of QUIJOTE, we have detected 1591 features above the 1 mK level (5σ below 42 GHz). Of these lines, 188 remain unidentified. We note, however, that the number of unknown spectral features above the 3σ level is much larger. Future improved QUIJOTE data will permit us to confirm them. Only four of these unidentified lines have intensities above 3 mK. The frequencies of these four lines are, in addition, in perfect harmonic relation with J_u = 7, 8, 9, 10. They are shown in Fig. 1 and their line parameters are given in Table 1. They do not show any hyperfine structure, and no other nearby lines are present with similar intensities. This discards a symmetric rotor, or a linear radical, as possible carrier. This is therefore a linear molecule with a $^1\Sigma$ ground electronic state, or with a slightly asymmetric rotor with electronic state ^1A. By fitting the observed frequencies to the standard Hamiltonian for a linear molecule ($\nu(J \rightarrow J-1) = 2B_0J - 4D_0J^3$), we derived B_0 = 2411.94397 ± 0.00055 MHz and D_0 = 138 ± 3 Hz. The standard deviation of the fit is 4.4 kHz. The possibility that these four strong lines appear by chance in harmonic relation with this precision is negligible. This means that we have detected a new molecular species in TMC-1.

The rotational constants B and D of the new species are very close to those of C_5H, for which B = 2395.131 ± 0.001 MHz and D = 127.41 ± 0.03 Hz (Cernicharo et al. 1986a,b, 1987; Gottlieb et al. 1986; McCarthy et al. 1999). The lack of fine or hyperfine structure permits us to exclude radical molecules. Nevertheless, and in order to explore what type of candidates could fit the observed B and D, we note that C_4N has a rotational constant of 2424.36 MHz, but its ground electronic state is $^2\Pi_r$ (McCarthy et al. 2003); for C_4O, the rotational constant is 2351.26 MHz, but its electronic ground state is $^3\Sigma$ (Ohshima et al. 1995). Finally, the HC_4O species is also a radical, with a rotational constant of 2279.91 MHz (Kohguchi et al. 1994). The rotational constant of species containing a sulphur atom such as HC_3S^+ is too large, B = 2735.46 MHz (Cernicharo et al. 2021d). The same holds for NCCS, which is a bent radical with $(B + C)/2$ = 2829.36 MHz (Nakajima et al. 2003). Concerning asymmetric species, HNCCS has been calculated to have an electronic ground state ^1A (Gronowski & Kolos 2015), and it is an isomer 147 kJ mol^{-1} above of HCSCN, a molecule recently detected in TMC-1 with QUIJOTE (Cernicharo et al. 2021f). However, although it is slightly asymmetric (A = 617.9 GHz), the value calculated by Gronowski & Kolos (2015) for $(B + C)/2$ is 2563 MHz, which represents a deviation of 6.3% with respect to the rotational constant of our species. The possibility that the lines belong to an isotopolog ^{13}C, ^{34}S, or D of an abundant species harboring line intensities above 300 mK (corresponding to a ^{13}C substitution) or 100 mK (for a ^{34}S or D substitution) is discarded from the analysis of all abundant species that were previously identified in the QUIJOTE data. It therefore appears that the carrier could contains five carbon atoms, or four carbon

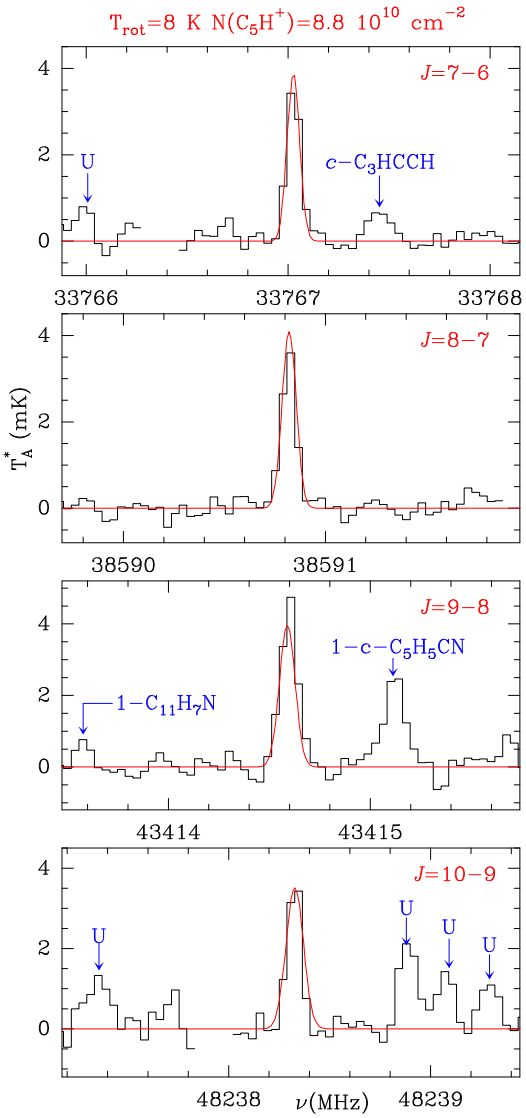

Fig. 1. Observed lines of C_5H^+ toward TMC-1. Line parameters are given in Table 1. The abscissa corresponds to the rest frequency assuming a local standard of rest velocity of 5.83 km s^{-1}. The ordinate is the antenna temperature corrected for atmospheric and telescope losses in mK. The red line shows the synthetic spectrum derived for T_{rot} = 8 K and N(C_5H^+) = 8.8×10^{10} cm^{-2}. Blank channels correspond to negative features produced in the folding of the frequency-switching data.

[3] http://www.iram.fr/IRAMFR/GILDAS

Table 1. Observed lines of C_5H^+ in TMC-1.

Transition	ν_{obs} [(a)]	$\nu_{obs} - \nu_{cal}$ [(b)]	$\int T_A^* \, dv$ [(c)]	Δv [(d)]	T_A^* [(e)]
7 – 6	33767.026 ± 0.005	−0.2	2.87 ± 0.18	0.74 ± 0.06	3.65 ± 0.16
8 – 7	38590.818 ± 0.005	−2.8	2.60 ± 0.12	0.67 ± 0.04	3.66 ± 0.17
9 – 8	43414.594 ± 0.005	5.1	3.39 ± 0.17	0.69 ± 0.04	4.60 ± 0.21
10 – 9	48238.325 ± 0.005	−2.2	2.28 ± 0.24	0.54 ± 0.07	3.98 ± 0.41

Notes. [(a)]Observed frequency assuming a v_{LSR} of 5.83 km s^{-1}. [(b)]Observed minus calculated frequencies in kHz. [(c)]Integrated line intensity in mK km s^{-1}. [(d)]Line width at half-intensity derived by fitting a Gaussian function to the observed line profile (in km s^{-1}). [(e)]Antenna temperature in millikelvin.

atoms and one nitrogen or oxygen atom. The only species that could fit these requirements are C_5H^+ and C_5H^- as all the other plausible candidates with O or N are open shell species. It might be argued that the carrier could be one of the anions of these radicals. However, none of the neutral radical species quoted previously has been detected in TMC-1. Moreover, molecules with a single sulphur atom do not fit the derived rotational constant.

Quantum chemical calculations by Botschwina (1991) provided a rotational constant for C_5H^+ of $B_0 = 2405 \pm 5$ MHz, and a proton affinity for C_5 of 860 ± 5 kJ mol^{-1}. A value of B_e for this species of ∼2420 MHz was obtained by Aoki (2014). More recent calculations by Bennedjai et al. (2019) provided a value for B_e of 2391.7 MHz. To obtain accurate spectroscopic parameters, we performed ab initio calculations for C_5H^+ and also for the C_5H species, for which the rotational parameters were experimentally determined. In this manner, we can scale the calculated values for the C_5H^+ species using experimental/theoretical ratios derived for the related species C_5H. This procedure has been found to provide rotational constants with an accuracy better than 0.1% (e.g., Cabezas et al. 2021). The geometry optimization calculations for all the species were made using the coupled cluster method with single, double, and perturbative triple excitations with an explicitly correlated approximation (CCSD(T)-F12; Knizia et al. 2009) and all electrons (valence and core) correlated together with the Dunning correlation consistent basis sets with polarized core-valence correlation triple-ζ for explicitly correlated calculations (cc-pCVTZ; Hill et al. 2010). These calculations were carried out using the Molpro 2020.2 program (Werner et al. 2021). The values for the centrifugal distortion constants were obtained using harmonic vibrational frequency calculations, with the second-order Møller-Plesset perturbation theory method (MP2; Møller & Plesset 1934) and the correlation consistent with polarized valence triple-ζ basis set (cc-pVTZ; Woon & Dunning 1993). These calculations were carried out using the Gaussian09 program (Frisch et al. 2016). The derived results are presented in Table 2.

The comparison of the calculated and experimental rotational constant for C_5H species reveals the good accuracy of the ab initio calculations we employed. The differences between the calculated B_e value and the experimental value is about 0.2% for C_5H. The scaled value for C_5H^+ is 2410.3 MHz, which matches the observed rotational constant very well, the difference is 0.07%. The scaled value for the distortion constant C_5H^+ also reproduces the D value derived from the TMC-1 lines remarkably well. Hence, our ab initio calculations provide conclusive arguments for the spectroscopic identification of C_5H^+ using our sensitive QUIJOTE survey of TMC-1. Using the B_e value calculated by Bennedjai et al. (2019) for C_5H, and correcting B_e of C_5H^+ by their ratio $B_{obs}(C_5H)/B_e(C_5H)$, we found $B_0(C_5H^+) \sim$ 2408.3 MHz, which also agrees well with our experimental rotational constant.

The other species that might fit the observed rotational constant is C_5H^-. However, there is a significant controversy about the nature of the ground state of this species. Two-color photodetachment studies by Tulej et al. (2011) suggested that the ground state is $^3\Sigma^-$ with a linear structure and a rotational constant of 2476.3 ± 6 MHz. In addition, the reported experimental value for the C_5H^- ($^3\Sigma^-$) species differs by more than 100 MHz from the predicted values obtained by Bennedjai et al. (2019) and our scaled value (Table 2). Moreover, if that assignment were correct, C_5H^- could not be the carrier of the observed lines as significant hyperfine structure is expected due to the spin 1/2 of H and the low spin-spin interaction constant derived, $\lambda = 7200 \pm 4500$ MHz. Consequently, the transitions with $J_u = N_u + 1$ and $J_u = N_u - 1$ will be close to those corresponding to $J_u = N_u$, and the $J_u = N_u + 1$ lines should be stronger than those with $J_u = N_u$. No lines with such a pattern are observed in our survey. Hence, we discard this putative state of C_5H^- as the carrier of our lines. There is also an additional caveat for this triplet linear C_5H^-. All linear anions detected so far in space have B(anion)< B(neutral). However, for the molecule observed by Tulej et al. (2011), the situation is the opposite, B(anion)> B(neutral). Additional controversy arises from the recent calculations of Bennedjai et al. (2019). They concluded that the ground electronic state of C_5H^- contains a C_3 ring with very different rotational constants than those observed. In addition, they also provided strong arguments against the viability of the triplet linear form as it is very dependent on the electron correlation energy, which denotes instability for this state. Hence, the ring ground electronic state of C_5H^-, although potentially expected in TMC-1, is not the carrier of our lines. We note, however, that they also computed a second slightly asymmetric isomer for this anion. It is 0.7 eV above the ring structure, with rotational constants $A_0 \sim 793$ GHz, and $(B+C)/2 \sim 2395.2$ MHz. This bent ^1A isomer could also fit the observed rotational constant. Our calculations predict a scaled value for $(B+C)/2 \sim 2395.5$ MHz (see Table 2).

All the anions that were detected in TMC-1 were also observed in the envelope of the carbon-rich star IRC+10216. We have explored the recent survey of this source performed with the Yebes 40 m radio telescope (Pardo et al. 2022) and found no emission at the frequencies of the four lines of TMC-1. We also searched in the available data from the IRAM 30 m telescope at 3 mm and 2 mm for lines in these ranges without success. Although this is not a definitive argument, it is an important drawback for bent-C_5H^- (^1A) being the carrier of the lines. Finally, although C_3H^+ has been found only in PDRs and diffuse media so far (Pety et al. 2012; McGuire et al. 2013, 2014; Cuadrado et al. 2015; Gúzman et al. 2015; Gerin et al. 2019; Tercero et al. 2020), its presence in TMC-1 could be a solid argument to assign C_5H^+ as carrier of the U-lines. Using the QUIJOTE data, a very nicely detected line ($S/N \sim 10$) appears just at the predicted frequency of the $J = 2 - 1$ transition of C_3H^+.

Table 2. Theoretical spectroscopic parameters for the different molecular candidates for the observed lines in TMC-1 (all in MHz).

		C_5H^+ ($^1\Sigma$)		l-C_5H^- ($^3\Sigma$)		ql-C_5H^- (^1A)		C_5H ($^2\Pi$)	
Parameter	TMC-1 [a]	Calc. [b]	Scaled [c]	Calc. [b]	Scaled [c]	Calc. [b]	Scaled [c]	Exp. [d]	Calc. [b]
B_e	2411.94397(55)	2404.2	2410.3	2366.4	2372.4	2389.5	2395.5 [e]	2395.131(1)	2389.1
$D \times 10^{-6}$	138(3)	102	127	97.9	121	101	126	127.41(3)	103

Notes. [a]Parameters derived using the TMC-1 frequencies from Table 1. [b]This work; see text. [c]This work; scaled by the ratio Exp/Calc. of the corresponding parameter for C_5H species. [d]Cernicharo et al. (1986a,b, 1987), Gottlieb et al. (1986), McCarthy et al. (1999). [e]$(B + C)/2$.

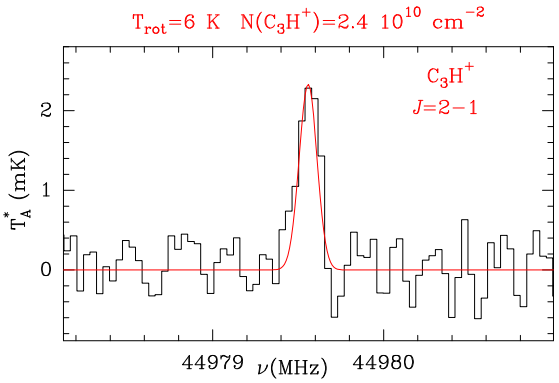

Fig. 2. Observed $J = 2 - 1$ line of C_3H^+ toward TMC-1. The abscissa corresponds to the rest frequency assuming a local standard of rest velocity of 5.83 km s^{-1}. The ordinate is the antenna temperature corrected for atmospheric and telescope losses in mK. The red line shows the synthetic spectrum derived for $T_{rot} = 6$ K and $N(C_3H^+) = 2.4 \times 10^{10}$ cm^{-2}.

The line is shown in Fig. 2. This represents the first detection of this cation in a cold starless core and provides key information about the chemistry of C_3H^+ in cold and dense environments. Moreover, the observation of the $J = 2 - 1$ line of C_3H^+ in emission rules out a previous tentative identification of this species in TMC-1 based on a noisy absorption feature at the frequency of this same transition (McGuire et al. 2013).

Adopting C_5H^+ as carrier of the U-lines, a model line profile fitting procedure provides a rotational temperature of 8 ± 1 K and a column density of $(8.8 \pm 0.5) \times 10^{10}$ cm^{-2}. We assumed a dipole moment value of 2.88 D (Botschwina 1991). The computed synthetic line spectra are shown in Fig. 1 and fit the observed line intensities and profiles very well. We adopted a line width of 0.6 km s^{-1} and a uniform brightness source of diameter 80″ (Fossé et al. 2001). For C_3H^+ we have only one line, and we adopted a rotational temperature of 6 K, which provides a column density for this species of $(2.4 \pm 0.2) \times 10^{10}$ cm^{-2}. When we assume a column density for H_2 of 10^{22} cm^{-2} (Cernicharo & Guélin 1987), the abundances of C_5H^+ and C_3H^+ are $(8.8 \pm 0.5) \times 10^{-12}$ and $(2.4 \pm 0.2) \times 10^{-12}$, respectively. The abundance ratio of the two species is 3.5 ± 0.5.

4. Discussion

To investigate the chemistry behind the formation of C_3H^+ and C_5H^+, we built a pseudo-time-dependent gas-phase chemical model of a cold dark cloud using a chemical network largely based on the RATE12 network from the UMIST database (McElroy et al. 2013). The model is similar to the models presented by Agúndez et al. (2015), Marcelino et al. (2020), and Cabezas et al. (2022b). The results from the chemical model are shown in Fig. 3, where one should focus on the so-called early time (10^5–10^6 yr), at which calculated and observed abundances in TMC-1 show the best overall agreement (see, e.g., Agúndez & Wakelam 2013). The pure carbon clusters with an odd number of carbon atoms C_3, C_5, and C_7 are calculated to be abundant. In particular, C_3 is predicted to be very abundant, with a peak abundance as high as $\sim 10^{-5}$ relative to H_2. The carbon clusters C_5 and C_7 have calculated peak abundances in the range 10^{-9}–10^{-8} relative to H_2. For these neutral carbon clusters, the chemical model indicates that the larger the size, the lower the abundance. In the case of the ions C_3H^+, C_5H^+, and C_7H^+, which can be seen as the protonated forms of C_3, C_5, and C_7, respectively, their calculated early-time abundances do not show the trend of decreasing abundance with increasing size. In fact, the smallest member, C_3H^+, has the lowest calculated abundance, while the medium-sized ion C_5H^+ shows the highest abundance. This is in agreement with the observations of TMC-1, which indicate that C_5H^+ is more abundant than C_3H^+. The underlying reason of this behavior is the different reactivity of C_3H^+ and C_5H^+ with H_2.

In a simplified chemical scheme, protonated molecules are mostly formed by proton transfer to the corresponding neutral counterpart, while they are mainly destroyed through dissociative recombination with electrons (e.g., Agúndez et al. 2015). However, in the case of the protonated forms of the carbon clusters C_3, C_5, and C_7, the behavior is somewhat different. Moreover, the chemical processes of formation and destruction are very different for C_3H^+ and for the larger analogs C_5H^+ and C_7H^+. The underlying reasons are that the abundance of C_3 is far higher than that of C_5 and C_7, and the reactivity of C_3H^+ with H_2 is far stronger than that of C_5H^+ and C_7H^+. According to the chemical model, C_3H^+ is mainly formed through proton transfer from HCO^+ and H_3O^+ to C_3, following the usual pathway of many other protonated molecules. However, the main destruction process of C_3H^+ does not involve the dissociative recombination with electrons, but the reaction with H_2. This reaction occurs fast through radiative association, leading to the linear and cyclic isomers of the ion $C_3H_3^+$, which are key intermediates in the synthesis of C_3H_2 isomers (see, e.g., Loison et al. 2017). In the cases of C_5H^+ and C_7H^+, the main formation pathways do not involve proton transfer to C_5 and C_7, but other ion-neutral reactions such as $C_5^+ + H_2$, $C^+ + C_4H_2$, and $C + C_4H_2^+$ in the case of C_5H^+, and $C_7^+ + H_2$, $C^+ + C_6H_2$, and $C + C_6H_2^+$ for C_7H^+. In the case of C_3H^+, the high abundance of C_3 makes the route involving proton transfer very efficient, while the lower abundances of C_5 and C_7 make the proton transfer pathways less efficient than other ion-neutral routes. The destruction of C_5H^+ and C_7H^+ is different from that of C_3H^+ because the former shows a much lower reactivity with H_2 than the latter. As a consequence, C_5H^+ and C_7H^+ are mostly destroyed through dissociative recombination with electrons and reaction with neutral atoms, as occurs for many other protonated molecules. The different chemistry of C_3H^+, compared to that of C_5H^+ and C_7H^+

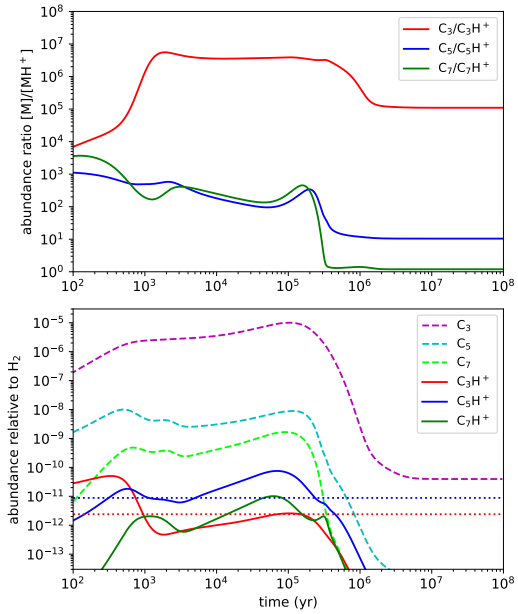

Fig. 3. Chemical models for the C_nH^+ species. *Upper*: computed abundance ratio between the clusters C_3, C_5 and C_7 and their protonated forms C_nH^+ as a function of time. *Lower*: abundances relative to H_2 for the carbon clusters and their protonated derivatives. The dotted horizontal lines correspond to the abundances observed in TMC-1 for C_3H^+ and C_5H^+.

directly translates into the calculated abundances and neutral-to-protonated abundance ratios. While the calculated C_5/C_5H^+ and C_7/C_7H^+ ratios are in the range 1–10^3 found for other protonated molecules (e.g., Agúndez et al. 2015; Cernicharo et al. 2020a; Cabezas et al. 2022b), the calculated C_3/C_3H^+ is much higher (see the top panel in Fig. 3). Moreover, the calculated abundance of C_3H^+ remains below that of C_5H^+. It is worth noting, however, that in spite of the reactivity of C_3H^+ with H_2, its calculated abundance does not drop to negligible levels because the abundance of its main precursor, the carbon cluster C_3, is very high.

Last, if we trust the chemical model, then it is predicted that C_7H^+ should be present in TMC-1 as well, with an abundance a few times below that of C_5H^+. The current sensitivity of the QUIJOTE line survey, however, does not allow us to identify C_7H^+, but the improvement in the sensitivity planned for the coming years could allow us to detect this species and confirm the above chemical scenario.

5. Conclusions

We reported the discovery of the cation C_5H^+ in TMC-1. We also reported the first detection of the cation C_3H^+ in a cold starless core. It was previously only observed in the direction of PDRs and diffuse interstellar clouds. The assignment of the four observed, harmonically related lines, to C_5H^+ was based on accurate ab initio calculations, which permit us to rule out C_5H^- as the possible carrier of these lines. Our chemical model reproduces the observations satisfactorily and explains the lower abundance of C_3H^+ with respect to C_5H^+ as due to the much higher reactivity of the former with respect to the latter. C_7H^+ is predicted to have an abundance a few times below that of C_5H^+. It might therefore be detectable with future QUIJOTE data with a higher signal-to-noise ratio.

Acknowledgements. We thank ERC for funding through grant ERC-2013-Syg-610256-NANOCOSMOS. M.A. thanks MICIU for grant RyC-2014-16277. We also thank Ministerio de Ciencia e Innovación of Spain (MICIU) for funding support through projects PID2019-106110GB-I00, PID2019-107115GB-C21/AEI/10.13039/501100011033, and PID2019-106235GB-I00.

References

Agúndez, M., & Wakelam, V. 2013, Chem. Rev., 113, 8710
Agúndez, M., Cernicharo, J., Guélin, M., et al. 2010, A&A, 517, L2
Agúndez, M., Cernicharo, J., de Vicente, P., et al. 2015, A&A, 579, L10
Agúndez, M., Cabezas, C., Tercero, B., et al. 2021, A&A, 647, L10
Aoki, K. 2014, Ad. Space Res., 54, 1651
Bennedjai, S. C., Hammoutène, D., & Senent, M. L. 2019, ApJ, 871, 255
Botschwina, P. 1991, J. Chem. Phys., 95, 4360
Brünken, S., Gupta, H., Gottlieb, C. A., et al. 2007, ApJ, 664, L43
Cabezas, C., Agúndez, M., Marcelino, N., et al. 2021, A&A, 654, A45
Cabezas, C., Agúndez, M., Marcelino, N., et al. 2022a, A&A, 657, L4
Cabezas, C., Agúndez, M., Marcelino, N., et al. 2022b, A&A, submitted
Cernicharo, J. 1985, Internal IRAM report (Granada: IRAM)
Cernicharo, J. 2012, in ECLA 2011: Proc. of the European Conference on Laboratory Astrophysics, eds. C. Stehl, C. Joblin, & L. d'Hendecourt (Cambridge: Cambridge Univ. Press), EAS Publ. Ser., 251, https://nanocosmos.iff.csic.es/?page_id=1619
Cernicharo, J., & Guélin, M. 1987, A&A, 176, 299
Cernicharo, J., Kahane, K., Gómez-Gónzalez, J., & Guélin, M. 1986a, A&A, 164, L1
Cernicharo, J., Kahane, K., Gómez-Gónzalez, J., & Guélin, M. 1986b, A&A, 167, L5
Cernicharo, J., Guélin, M., & Walmsley, C. M. 1987, A&A, 172, L5
Cernicharo, J., Guélin, M., Agúndez, M., et al. 2007, A&A, 467, L37
Cernicharo, J., Guélin, M., Agúndez, M., et al. 2008, ApJ, 688, L83
Cernicharo, J., Marcelino, N., Agúndez, M., et al. 2020a, A&A, 642, L17
Cernicharo, J., Marcelino, N., Pardo, J. R., et al. 2020b, A&A, 641, L9
Cernicharo, J., Agúndez, M., Kaiser, R., et al. 2021a, A&A, 652, L9
Cernicharo, J., Cabezas, C., Agúndez, M., et al. 2021b, A&A, 647, L3
Cernicharo, J., Agúndez, M., Cabezas, C., et al. 2021c, A&A, 649, L15
Cernicharo, J., Cabezas, C., Endo, Y., et al. 2021d, A&A, 646, L3
Cernicharo, J., Cabezas, C., Bailleux, S., et al. 2021e, A&A, 646, L7
Cernicharo, J., Cabezas, C., Endo, Y., et al. 2021f, A&A, 650, L14
Cuadrado, S., Goicoechea, J. R., Pilleri, P., et al. 2015, A&A, 575, A82
Fossé, D., Cernicharo, J., Gerin, M., & Cox, P. 2001, ApJ, 552, 168
Frisch, M. J., Trucks, G. W., Schlegel, H. B., et al. 2016, Gaussian 16 Revision A.03
Gerin, M., Liszt, H., Neufeld, D., et al. 2019, A&A, 622, A26
Gottlieb, C. A., Gottlieb, E. W., & Thaddeus, P. 1986, A&A, 164, L5
Gronowski, M., & Kolos, R. 2015, J. Mol. Struct., 1090, 76
Gúzman, V. V., Pety, J., Goicoechea, J. R., et al. 2015, ApJ, 800, L33
Hill, J. G., Mazumder, S., & Peterson, K. A. 2010, J. Chem. Phys., 132, 054108
Kawaguchi, K., Fujimori, R., & Aimi, S. 2007, PASJ, 59, L47
Knizia, G., Adler, T. B., & Werner, H.-J. 2009, J. Chem. Phys., 130, 054104
Kohguchi, H., Ohshima, Y., & Endo, Y. 1994, J. Chem. Phys., 101, 6463
Loison, J.-C., Agúndez, M., Wakelam, V., et al. 2017, MNRAS, 470, 4075
Marcelino, N., Agúndez, M., Tercero, B., et al. 2020, A&A, 643, L6
McCarthy, M. C., Chen, W., Apponi, A. J., et al. 1999, ApJ, 520, 158
McCarthy, M. C., Fuchs, G. W., Kucera, J., et al. 2003, J. Chem. Phys., 118, 3549
McCarthy, M. C., Gottlieb, C. A., Gupta, H. C., et al. 2006, ApJ, 652, L141
McElroy, D., Walsh, C., Markwick, A. J., et al. 2013, A&A, 550, A36
McGuire, B. A., Carroll, P. B., Loomis, R. A., et al. 2013, ApJ, 774, 56
McGuire, B. A., Carroll, P. B., Sanders, J. L., et al. 2014, MNRAS, 442, 2901
Møller, C., & Plesset, M. S. 1934, Phys. Rev., 46, 618
Müller, H. S. P., Schlöder, F., Stutzki, J., & Winnewisser, G. 2005, J. Mol. Struct., 742, 215
Nakajima, M., Sumiyoshi, Y., & Endo, Y. 2003, J. Chem. Phys., 118, 7803
Ohshima, Y., Endo, Y., & Ogata, T. 1995, J. Chem. Phys., 102, 1493
Pickett, H. M., Poynter, R. L., Cohen, E. A., et al. 1998, J. Quant. Spectr. Rad. Transf., 60, 883
Pardo, J. R., Cernicharo, J., & Serabyn, E. 2001, IEEE Trans. Antennas Propag., 49, 12
Pardo, J. R., Cernicharo, J., Tercero, B., et al. 2022, A&A, in press https://doi.org/10.1051/0004-6361/202142263
Pety, J., Gratier, P., Guzmán, V., et al. 2012, A&A, 548, A68
Remijan, A. J., Hollis, J. M., Lovas, F. J., et al. 2007, ApJ, 664, L47
Thaddeus, P., Gottlieb, C. A., Gupta, H., et al. 2008, ApJ, 677, 1132
Tercero, B., Cernicharo, J., Cuadrado, S., et al. 2020, A&A, 636, L7
Tercero, F., López-Pérez, J. A., Gallego, J. D., et al. 2021, A&A, 645, A37
Tulej, M., Mazzotti, F. J., & Maier, J. P. 2011, J. Phys. Chem. A, 115, 6878
Werner, H. J., Knowles, P. J., Knizia, G., et al. 2021, MOLPRO, version 2021.3
Woon, D. E., & Dunning, T. H., Jr 1993, J. Chem. Phys., 98, 1358